Journal of Experimental Pharmacology

Dovepress
Taylor & Francis Group

Open Access Full Text Article

ORIGINAL RESEARCH

Anti-Tyrosinase and Radical Scavenging Activities of Selected Cassipourea Plants and Isolated 7-Methoxygeranin A: Traditional Use as Skin Lighteners

Nomakhosi Mpofana[1,2], Michael Paulse[3], Masande Yalo[4], Ncoza Cordelia Dlova[1], Ahmed Hussein[4], Adedayo Ayodeji Lanrewaju[5], Halimat Yusuf Lukman[5], Jamiu Olaseni Aribisala[5], Fanie Rautenbach[6], Jeanine L Marnewick[6], Saheed Sabiu[5]

[1]Dermatology Department, Nelson R. Mandela School of Medicine, University of Kwazulu-Natal, Durban, 4000, South Africa; [2]Department of Somatology, Durban University of Technology, Durban, 4000, South Africa; [3]Graduate School of Business, The University of Cape Town, Cape Town, 8000, South Africa; [4]Department of Chemistry, Cape Peninsula University of Technology, Cape Town, 8000, South Africa; [5]Department of Food and Biotechnology, Durban University of Technology, Durban, 4000, South Africa; [6]Applied Microbial and Health Biotechnology Institute, Cape Peninsula University of Technology, Cape Town, South Africa

Correspondence: Nomakhosi Mpofana, Dermatology Department, Nelson R. Mandela School of Medicine, University of KwaZulu-Natal, Durban, 4000, South Africa, Tel +27786087119, Email nomakhosim@dut.ac.za

Journal of Experimental Pharmacology downloaded from https://www.dovepress.com/
For personal use only.

Background: In rural areas of KwaZulu-Natal and Eastern Cape Provinces, South Africa, women have traditionally used bark extracts from *Cassipourea flanaganii, C. malosana*, and *C. gummiflua* for skin lightening and sun protection. This study investigates the anti-tyrosinase and antioxidant activities of methanolic bark extracts from these species, aiming to validate their traditional use and identify potential lead compounds for the treatment of skin hyperpigmentation.

Methods: Anti-tyrosinase activity was evaluated using half-maximal inhibitory concentration (IC_{50}) values, and antioxidant capacity was measured through FRAP, DPPH, and TEAC assays. Polyphenol and flavanol contents were quantified using Folin-Ciocalteu method. Potential lead compounds were identified through molecular docking, pharmacokinetic analysis, and molecular dynamics (MD) simulations. Statistical analyses, including ANOVA and post-hoc tests, compared extract activities.

Results: *C. flanaganii* exhibited the most potent anti-tyrosinase activity (IC_{50}: 37.10 µg/mL), though statistical differences among species were non-significant. *C. gummiflua* showed the highest polyphenol (143.68 mg GAE/g) and flavanol (14.67 mg QE/g) content, correlating with superior antioxidant activity (FRAP: 526.07 µmol AAE/g; DPPH: 390.26 µmol TE/g; TEAC: 596.98 µmol TE/g). The isolated compound 7-methoxygeranin A demonstrated lower anti-tyrosinase activity (IC_{50}: 45.16 µg/mL) compared to *C. flanaganii* extract, suggesting the presence of more potent metabolites. Molecular docking and MD simulations identified emodin 6,8-dimethyl ether as a thermodynamically stable lead compound (binding free energy: −39.88 kcal/mol), interacting with key catalytic residues over 150 ns. The compound demonstrated prolonged residence at the active site of tyrosinase, indicating strong-binding stability.

Conclusion: While *C. flanaganii* demonstrated the strongest anti-tyrosinase activity, C. gummiflua showed the highest antioxidant potential. Emodin 6,8-dimethyl ether emerged as a promising candidate for skin-lightening applications, warranting further in vitro and in vivo validation. These findings support the traditional use of *Cassipourea* species and highlight their potential for developing natural skin health products. Further studies are needed to explore the pharmacokinetics, safety, and efficacy of these compounds in clinical settings.

Keywords: anti-tyrosinase activity, antioxidant capacity, *Cassipourea* species, hyperpigmentation, molecular dynamics simulation, skin-lightening agents

Introduction

There is a long history of the use of natural remedies or plant-derived botanicals by various cultures. This use is encouraged by the medicinal properties of these plants[1,2] hence, they are considered ideal for pharmacological research.[3,4] Natural remedies

Received: 21 November 2024
Accepted: 8 March 2025
Published: 31 May 2025

© 2025 Mpofana et al. This work is published and licensed by Dove Medical Press Limited. The full terms of this license are available at https://www.dovepress.com/terms.php and incorporate the Creative Commons Attribution – Non Commercial (unported, v4.0) License (http://creativecommons.org/licenses/by-nc/4.0/). By accessing the work you hereby accept the Terms. Non-commercial uses of the work are permitted without any further permission from Dove Medical Press Limited, provided the work is properly attributed. For permission for commercial use of this work, please see paragraphs 4.2 and 5 of our Terms (https://www.dovepress.com/terms.php).

are gaining popularity owing to their easy access, cost-effectiveness, and safety compared to costly, synthetic, and pharmaceutical products.[5] The investigation of natural remedies such as tyrosinase inhibitors offers potential for the treatment of epidermal hyperpigmentation disorders owing to their pharmacological properties.[6,7]

Tyrosinase, a copper-containing enzyme, plays a crucial role in melanin biosynthesis within melanocytes, specialized cells found in the eyes, skin, and hair follicles.[8] Melanin determines eye, skin, and hair colour while also protecting against UV radiation and neutralizing free radicals in humans and other mammals.[8,9] Dysregulated tyrosinase activity can lead to excessive melanin production, causing hyperpigmentation disorders like melasma, solar melanosis, ephelides, acne scars, and senile lentigo.[10] The enzyme catalyses melanin synthesis through two key reactions:[11–14]

1. **O-Hydroxylation of Monophenols**: Tyrosinase converts tyrosine or 3,4-dihydroxyphenylalanine (L-DOPA) into diphenols by adding a hydroxyl group to the ortho position of the phenolic ring. For instance, tyrosine is hydroxylated to L-DOPA, which is further converted to dopaquinone.

Monophenol+O_2→TyrosinaseO-Diphenol+H_2O Monophenol+O_2 Tyrosinase O-Diphenol+H_2O

1. **Oxidation of O-Diphenols to O-Quinones**: Tyrosinase oxidizes o-diphenols into o-quinones by removing two electrons and protons, creating a double bond in the benzene ring.

O-Diphenol+O_2→TyrosinaseO-Quinone+H_2O O-Diphenol+O_2 Tyrosinase O-Quinone+H_2O

These reactions are followed by non-enzymatic steps where o-quinones undergo cyclization and polymerization to form melanin pigments. The melanin is packaged into melanosomes within melanocytes and transferred to keratinocytes, contributing to pigmentation and UV protection.[11–14]

UV radiation induces oxidative stress, activating melanogenesis and increasing ROS, which damages DNA and promotes melanocyte proliferation.[3–5,14–17] Antioxidants, particularly plant-derived, can scavenge free radicals and reduce hyperpigmentation.[9–11] The free radical scavenging activity of antioxidants depends on their type and concentration, which vary among plant species.[18] A common method for evaluating antioxidant efficacy is the DPPH free radical scavenging assay.[3,10,15,17,19] The level of total phenolics and flavonoids correlates with free radical-scavenging and anti-tyrosinase activity. Higher antioxidant levels enhance both properties, making them potent agents against oxidative stress and hyperpigmentation.[19]

Botanical compounds with tyrosinase inhibitory activity offer significant potential for regulating melanin production and addressing hyperpigmentation.[20] Existing treatments for hypermelanosis disorders are often limited by suboptimal outcomes, including high recurrence rates, toxicity, low stability, poor skin penetration, and reduced efficacy.[21] Consequently, there is growing scientific interest in developing novel compounds for hyperpigmentation treatment. Screening plants with reported anti-tyrosinase properties may aid in identifying active, safe lead compounds with both tyrosinase modulatory and antioxidant activities, which could be valuable in treating hyperpigmentation.

In vitro studies serve as a crucial preliminary step in the drug discovery process, paving the way for subsequent preclinical and clinical evaluations. Computational studies complement this process by enabling the identification of lead compounds in plants or plant extracts.[22] While the anti-tyrosinase activities of certain plants have been documented, Zuo et al[23] highlighted the anti-tyrosinase and antioxidant activities of specific flavonoids through both in vitro experiments and molecular docking approaches. Despite these advancements, many plants remain underexplored for their potential as tyrosinase inhibitors. *Cassipourea* species, including *Cassipourea flanaganii, Cassipourea malosana*, and *Cassipourea germiflua*, contain key bioactive compounds such as lupeol, lynoside, cassipourol, decahydroretinol, and azelaic acid.[4] These species are traditionally used to treat hypermelanosis in rural areas of South Africa's Eastern Cape and KwaZulu-Natal provinces. Recent analyses have evaluated their anti-tyrosinase and free radical scavenging activities.[3,6] However, the holistic experimental anti-tyrosinase and free radical scavenging activities of *Cassipourea* and exploration of potential lead compounds responsible for these effects are limited. This study reports the in vitro tyrosinase and free radical inhibitory potential of three *Cassipourea* species and for the first time computationally screened and analyzed the binding interactions of lead tyrosinase modulators of

Cassipourea species. This study was carried out to fully decipher the anti-tyrosinase mechanism of action of *Cassipourea* species geared towards the discovery and development of an effective anti-tyrosinase drug candidate.

Materials and Methods

Reagents, Chemicals, and Solvents

All chemicals and reagents used were of an analytical grade. Sigma Aldrich in Cape Town, South Africa, supplied mushroom tyrosinase (EC 1.14.18.1) with an activity of 5771 units/mg, as well as L-tyrosine and kojic acid. Merck in Cape Town, South Africa, supplied organic solvents such as methanol (MeOH), ethanol (EtOH), hexane, dichloromethane (DCM), ethyl acetate (EtOAc), and dimethyl sulfoxide (DMSO). Thin layer chromatography (TLC) was carried out on normal-phase silica gel 60 PF_{254} pre-coated aluminum plates from Merck in Cape Town, South Africa.

Plant Material

Three *Cassipourea* plants were collected from Kwa Madiba in Bizana and from Pirie Forests in Qonce. Professor Neil Crouch, a botanist at the South African National Biodiversity Institute (SANBI), identified leaf material from the sampled plants. Voucher specimens were deposited at the Durban's KwaZulu-Natal Herbarium (NH). The Department of Forestry, Fisheries, and the Environment (DFFE) (12/11/1/7A (JD)) granted the first author (NM) a permit to harvest the stem bark material.

Identification of Plant Material

The identified plant materials collected by N. Mpofana are listed, along with their respective collector codes and numbers in Table 1. The table provides essential information for the identification and reference of the plant materials used in this study.

Preparation of Extracts

The stem bark of the plant (100 g) was blended and extracted with 70% methanol (1:7 ratio wt/vol L) at room temperature (25°C) for 24 hours. The methanol extract was then filtered and dried under reduced pressure at 40°C. The concentrated extract was further processed under vacuum to eliminate excess methanol. This procedure was consistently applied to all plant materials used in the study.

Isolation of Compounds

The air-dried powdered stem bark of *C. malosana* (100 g) was exhaustively extracted with 70% MeOH, and the combined extracts were concentrated to dryness under reduced pressure at 40°C. The residue (6.2 g) was pre-absorbed on silica gel, loaded on CC, and fractionated successively using chloroform-methanol (95.5). (90:10), (85:15). Eight fractions were analyzed by TLC using CHC_3l: MeOH: H_2O (200:52:6). Similar fractions were combined together, which resulted in a pure compound.

In vitro Assessment of Antioxidant Activity

Total polyphenol, flavonol, and flavanol content assays were used to determine the antioxidant content of the three plant extracts. Free radical scavenging assays (FRAP, DPPH, and TEAC) were used to determine the antioxidant capacity of the three extracts.

Table 1 Identification of Plant Material: Collector, Collection Code, and Voucher Numbers for Three Cassipourea Species

Collector	Code	Number	Plant Name	Voucher Number
N Mpofana	2020	1	*Cassipourea gummiflua* Tul. verticillata (N.E.Br.) J. Lewis	NH0151948-0
N Mpofana	2021	2	*Cassipourea malosana* (Baker) Alston	NH0151949-0
N Mpofana	2022	4	*Cassipourea flanaganii* (Schinz) Alston	NH0151951-0

https://doi.org/10.2147/JEP.S504759

Total Polyphenol Determination

The total polyphenolic content was determined using the Folin–Ciocalteu method.[8] In a clear 96-well microplate, 25 µL of the sample was combined with 125 µL of 0.2 M Folin–Ciocalteu reagent. After 5 minutes, 100 µL of 7.5% aqueous Na_2CO_3 was added to each well. The plates were then incubated at room temperature for 2 hours before measuring the absorbance at 765 nm. A standard curve was created using gallic acid concentrations of 0, 20, 50, 100, 250, and 500 mg/L in 10% ethanol. The results were expressed as milligrams of gallic acid equivalents per gram of sample (mg GAE/g).

Flavonol Content Determination

The Flavonol content was determined using quercetin 0, 5, 10, 20, 40, and 80 mg/L in 95% ethanol as standard. In the sample wells of a clear 96-well plate, 12.5 µL of the crude sample extract was mixed with 12.5 µL 0.1% HCl in 95% ethanol, 225 µL 2% HCl, and incubated for 30 min at room temperature. The absorbance was measured at 360 nm at a temperature of 25°C.[9] The results are expressed as mg quercetin equivalent per g sample (mg QE/g). Flavanol content was determined using the method described by Treutter (1989).[10] Briefly, 50 µL of the sample was mixed with 250 µL 4-(Dimethylamino)-cinnamaldehyde (DMACA) (0.5 g/L (MeOH: HCl, 3:1)) in a 96-well clear plate. After incubation at room temperature for 15 min, absorbance was measured at 640 nm. A linear standard curve using 0, 0.2, 0.5, 1.0, 1.5, and 2.0 mg/mL catechin in methanol was constructed. The results are expressed as mg catechin equivalent per g sample (mg CE/g).

Ferric Reducing Antioxidant Power (FRAP) Assay

The FRAP assay was performed as described by Benzie and Strain (1999).[11] In a 96-well microplate, 10 µL of the crude sample extract was combined with 300 µL of the FRAP reagent, which consists of a 0.3 M acetate buffer at pH 3.6, 10 mm 2,4,6-tripyridyl-s-triazine (TPTZ) in 0.1 M HCl, and 20 mm iron (III) chloride hexahydrate ($FeCl_3 \cdot 6H_2O$), along with 6.6 mL of distilled water. This mixture was incubated for 30 minutes at 37°C in a plate reader, after which the absorbance was measured at a wavelength of 593 nm. L-Ascorbic acid was utilized as a standard, with concentrations ranging from 0 to 1000 µM. The results were expressed as micromoles of ascorbic acid equivalent per gram of sample (µM AAE/g).

2,2′-Azino-Di-3-Ethylbenzothiazoline Sulphonate (ABTS) Assay

ABTS assay was performed as described by Re et al (1999).[12] The stock solutions included 7 mM ABTS and 140 mM potassium peroxodisulfate ($K_2S_2O_8$). The working solution was prepared by adding 88 µL $K_2S_2O_8$ to 5 mL ABTS solution. The two solutions were mixed thoroughly and allowed to react for 24 h at room temperature in the dark. Trolox (6-Hydroxy-2,5,7,8-tetramethylchroman-2-carboxylic acid) was used as the standard at concentrations ranging between 0 and 500 µM. Sample extracts (25 µL) were allowed to react with 275 µL ABTS in the dark at room temperature for 30 min before the absorbance was read at 734 nm at 25°C in a plate reader. The results are expressed as µM trolox equivalent per g sample (µM TE/g).

1,1-Diphenyl-2-Picryl-Hydrazyl (DPPH) Assay

The DPPH assay was performed according to the method described by Sharma and Bhat (2009).[13] Sample extracts (25 µL) were allowed to react with 275 µL DPPH (prepared in methanol) in the dark at room temperature for 30 min before the absorbance was read at 517 nm at 25°C in a plate reader. The same standard used in the ABTS assay was also used in this assay. The results are expressed as µM trolox equivalent per g sample (µM TE/g).

Anti-Tyrosinase Inhibition Assay

The skin enzymatic inhibitory assay was executed following the approach used by Momtaz et al[14] and Souza et al.[15] Extracts and isolated compounds were dissolved in dimethyl sulfoxide (DMSO) to a final concentration of 20 mg/mL. The stock solutions were then diluted to 100 µg/mL and 200 µg/mL in 50 mm potassium phosphate buffer (pH 6.5). Kojic acid was used as a control agent [20]. In the wells of a 96-well plate, 70 µL of each sample dilution was mixed with 30 µL of tyrosinase (500 U/mL in phosphate buffer) in triplicates. After incubation at room temperature for 5 min, 110 µL of the substrate (2 mm L-tyrosine) was added to each well. Extracts and isolated compounds were dissolved in dimethyl sulfoxide (DMSO) to a final concentration of 20 mg/mL. The stock solutions were then diluted to

100 µg/mL and 200 µg/mL in 50 mm potassium phosphate buffer (pH 6.5). Kojic acid was used as a control drug [20]. In the wells of a 96-well plate, 70 µL of each sample dilution was combined with 30 µL of tyrosinase (500 U/mL in phosphate buffer) in triplicates. After incubation at room temperature for 5 min, 110 µL of the substrate (2 mm L-tyrosine) was added to each well. The final concentrations of the extracts, isolated samples, and positive controls ranged from 0.2 to 1000 µg/mL. Incubation commenced for 30 min at room temperature by measuring the absorbance at 490 nm with an AccuReader M965 Metertech (V1.11). Equation 1 was used to determine the percentage of tyrosinase inhibition. Incubation commenced for 30 minutes at room temperature with absorbance measured at 490 nm with an AccuReader M965 Metertech (V1.11). Equation 1 was used to determine the percentage of tyrosinase inhibition:

$$\%\text{Tyrosinase inhibition} = \frac{(A_{control} - A_{blank\,1}) - (A_{sample} - A_{blank\,2})}{(A_{control} - A_{blank})} \times 100\% \quad (1)$$

Where A_{control} is the absorbance of the control with the enzyme, A_{blank1} is the absorbance of the control without the enzyme, A_{sample} is the absorbance of the test sample with the enzyme and A_{blank2} is the absorbance of the test sample without the enzyme.

The half-minimal inhibitory concentration (IC_{50}) measures a sample's effectiveness in inhibiting biochemical function. The IC_{50} values were calculated using nonlinear regression analysis. The dose–response curve was generated by plotting the percentage inhibition versus the logarithm of the sample concentration. For determining the IC_{50} of the samples against tyrosinase, a dose–response curve with five concentrations (ranging from 1000 to 0.1 mg/mL) was utilized. All statistical analyses were conducted using the GraphPad Prism software, version 9.0.0 (121).[15]

In Silico Study

Drug-Likeness, Pharmacokinetics, and Toxicity Studies of Cassipourea Metabolites

The 17 metabolites previously identified in the three *Cassipourea* species,[16] 7-methoxygeranin A, and kojic acid (reference standard), were virtually screened for their oral drug-likeness [using the Lipinski rule of 5 (Ro5), which states that molecular weight, hydrogen bond donor (HBD), hydrogen bond acceptor (HBA), bioavailability, and octanol-water partition (Log P) must be ≤500 g/mol, 5, 10, 0.55, and 4.5, respectively], absorption, distribution, metabolism, and excretion properties by inserting a Simplified Molecular Input Line Entry System (SMILES) into the SwissADME server.[17] Toxicity prediction was carried out using the ProTox-II server (https://tox-new.charite.de/protox_II/) (accessed on July 30, 2024).[18]

Molecular Docking and Validation

The 3D structures of the identified metabolites of *Cassipourea*, 7-methoxygeranin A, and kojic acid were obtained from PubChem (https://pubchem.ncbi.nlm.nih.gov/) (accessed June 10, 2024), while the crystal structure of tyrosinase (2Y9W) was retrieved from the Protein Data Bank (https://www.rcsb.org/). The structures were optimized in preparation for docking using the UCSF chimera for the enzyme by removing all non-standard amino acids and water, and the Open Babel plugin of PyRx software for the metabolites by adding Gasteiger charges.[19] The amino acids at the binding pocket of the receptor were selected as previously reported[20] with the coordinate center (X = 3.83, Y = 27.11, Z = 96.14). The docking procedure was subsequently validated using the superimposition procedure to assess the ability of AutoDock to correctly reproduce the ligand position in the crystal structure of the protein. Superimposition showed the partial binding orientation of the top-ranked compounds in the binding pocket of the protein by interacting with four active site residues (Cys83, His85, His244, and Val283) of the protein (Figure 1).

Molecular Dynamics Simulation

The MD simulation was conducted as described previously[21] using the graphical processing unit (GPU) version of the AMBER 18 package of the Centre for High Performance Computing (CHPC) in Cape Town, South Africa. The study employed the AMBER 18 force field with the FF18SB variant, and the simulation was carried out as described by[22] with a restraint in hydrogen atom bonds using the SHAKE algorithm with the SPFP precision model and simulation step size of 2fs during the 150 ns simulation.[23] The post-dynamic analysis of the RMSD, root means square fluctuation (RMSF), solvent accessible surface area (SASA), radius of gyration (ROG), and number of hydrogen (H) bonds were performed

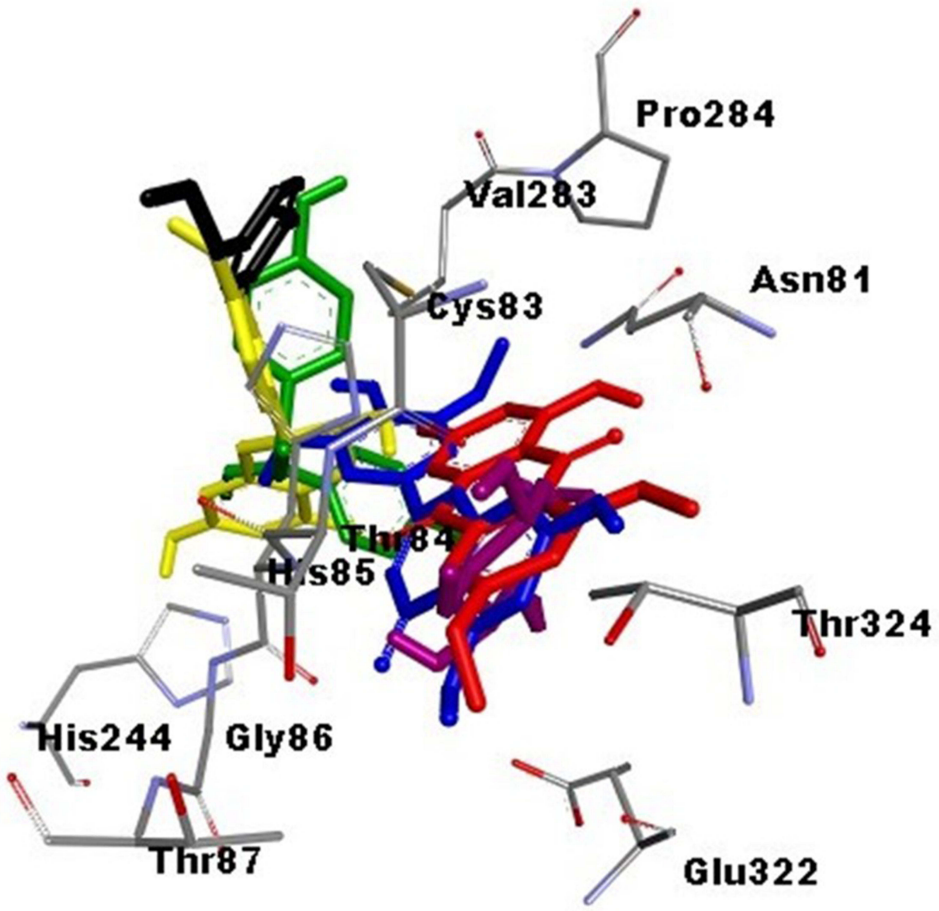


Figure 1 Docking validation via the superimposition of the docked top-ranked compounds [emodin 6,8-dimethyl ether (red), afzelechin (yellow), ellisinin A (green), tricin (blue), hexose (purple) and kojic acid (black)] at the active site of the crystal structure of tyrosinase.

using the CPPTRAJ module of the AMBER 18 suite, and their plots were obtained using Origin software V18 (Origin Lab Corporation, Northampton, MA, USA), while molecular mechanics with the generalized born surface area method [MM/GBSA] was used to obtain the energy components.[24] The 2D interaction plots of the resulting complexes were visualized using Discovery Studio version 21.1.0.[25]

Statistical Analyses

This section outlines the statistical tests employed and the rationale behind their selection. Jamovi (2024) software was used in the analysis. Descriptive statistics were utilized to summarize the key parameters measured in the antioxidant and anti-tyrosinase assays. Mean values, standard deviations and ranges were calculated to provide a clear overview of the distribution and variability of the data.

To compare the antioxidant activity of the three *Cassipourea* plant extracts, Analysis of Variance (ANOVA) was employed.[26–28] This statistical test allowed for the assessment of differences in antioxidant capacity among the extracts. Post-hoc tests, specifically Tukey's Honestly Significant Difference (HSD) test, were conducted to identify significant differences between pairs of groups.[29–31] The tyrosinase inhibitory activity of the *Cassipourea* plant extracts was compared using ANOVA. This analysis enabled the determination of whether there were significant differences in the inhibitory effects of the extracts on the enzyme.

In both ANOVA studies, the assumptions of homogeneity of variances were also assessed[32] using Levene's and Bartlett's tests.[33] In addition, the partial effect size (η^2p).[34–36] which measures the proportion of variance explained by a factor, reflecting the strength of association was also determined. Differences in activity are further assessed by

evaluating plots of the estimated marginal means (EMMs) which illustrates confidence intervals, predictability of variables, effect sizes among treatments and inference procedures for analyzing data.[37–40] By employing these statistical tests, we aimed to rigorously evaluate the antioxidant and anti-tyrosinase properties of the *Cassipourea* species and provide robust scientific evidence for their potential pharmacological applications.

Results

Identification of Plant Material

In Table 1, the identified plant materials collected by N. Mpofana are listed, along with their respective collector codes and numbers. These details provide essential information for the identification and reference of the plant materials used in this study.

Chemical Characterization

Fractionation of the ethanolic extract of *C. malosana* through column chromatography (CC) on silica gel and Sephadex LH-20 yielded compound **1** (Figure 2). Compound **1** (28.0 mg) was obtained as a brown powder directly from Fraction 3 of the main column after purification using Sephadex LH-20. Its chemical structure was determined by 1D (^{1}H, ^{13}C, and DEPT-135) and 2D (HSQC and HMBC) NMR spectroscopy (Figures S1–S7 Available form Figshare) and compared with the spectral data values of known compounds previously reported in the literature. It was subsequently identified as 7-methoxygeranin A based on the comparison of the results of MS and ^{1}H and ^{13}C-NMR spectroscopy with those of 7-methoxygeranin A reported previously from *C. gummiflua*[41] and *C. congoensis*.[42] The ^{1}H- and ^{13}C-NMR data for compound **1** are shown in Table S1.

Structural Elucidation of Compound 1

In the ^{1}H NMR spectrum of compound **1** (Table S1), three aromatic spin systems were observed: AM (ring A), formed by H-6 at δ_H 6.04, *d*, 2.1 *Hz* and H-8 at δ_H 6.05, d, 1.9 *Hz*; ABX (ring B), formed H-2′/6′ (δ_H 7.39, *d*, 8.6 *Hz*), and H-3′/5′ (δ_H 6.78, *d*, 8.7 *Hz*) and A ' B ' X ' (ring E), formed by H-2′/6′ (δ_H 7.39, *d*, 8.4 *Hz*), and H-3′/5′ (δ_H 6.78, *d*, 8.7 *Hz*). The H-6 and 8 doublets of the A ring protons were detected at δ_H 6.04, *d*, 2.1, *Hz* and 6.05, *d*, 1.9, *Hz* respectively. Two aliphatic spin systems were observed. One of them is in ring C, consisting of H-3 protons appearing at δ_H 3.91, *bd*, 3.0 *Hz*, and H-4 at δ_H 4.33, *bd*, 3.0 *Hz*. The second aliphatic spin system was observed in ring F and consisted of protons H-2′ appearing at δ_H 4.62, *d*, 8.0 *Hz*, H-3′ at δ_H 3.85, *m*; H-4′a at δ_H 2.74, *dd*, 16.3, 5.6 hz, and H-4′b at 2.43, *dd*, 16.3, 8.3

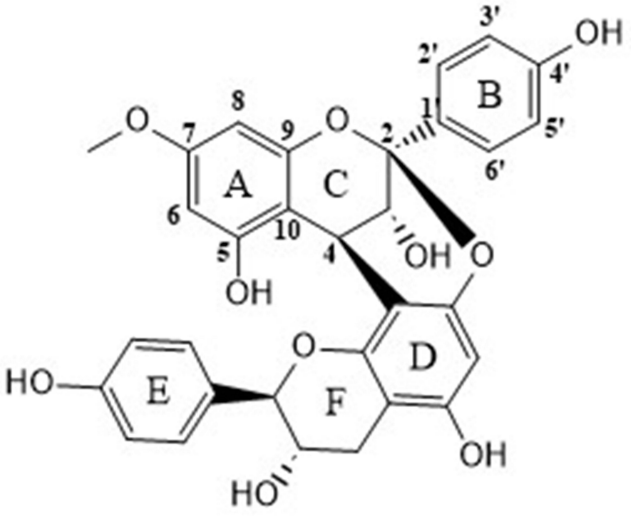


Figure 2 Chemical structure of the isolated compound from C. malosana.

https://doi.org/10.2147/JEP.S504759

Table 2 Illustration of Antioxidant Activity of Three Cassipourea Species

Code	Extract	Poly-Phenols (mg GAE/g)	Flavo-nols (mg QE/g)	Flava-nols (mg CE/g)	FRAP (µmol AAE/g)	DPPH (µmol TE/g)	TEAC (µmol TE/g)
2020	*C. gummiflua*	143.68 ± 7.26[a]	14.67 ± 3.02[a]	59.28 ± 0.65[a]	526.07 ± 24.00[a]	390.26 ± 18.80[a]	596.98 ± 13.30[a]
2021	*C. malosana*	100.01 ± 0.78[b]	5.21 ± 0.39[b]	33.79 ± 0.09[b]	362.68 ± 9.44[b]	292.37 ± 4.46[b]	381.97 ± 3.12[b]
2022	*C. flanaganii*	97.91 ± 0.96[b]	6.58 ± 0.48[b]	24.82 ± 0.11[c]	378.56 ± 11.60[b]	257.20 ± 5.46[c]	372.92 ± 3.82`
One-way ANOVA F-Statistic & p-values		*F*(2, 3.57) = 50.20 *p* =0.002	*F*(2, 3.13) = 13.00 *p* =0.031	*F*(2, 3.04) = 2969.00 *p* <0.001	*F*(2, 3.73) = 48.70 *p* =0.002	*F*(2, 3.16) = 40.40 *p* =0.006	*F*(2, 3.39) = 316.30 *p* <0.001

Notes: Values with different superscript letters (a, b, c) within the same column are significantly different ($p < 0.05$) based on one-way ANOVA followed by Tukey's HSD test.

Hz. These data indicate that compound **1** is a dimer consisting of two afzelechin units. Thus, based on the NMR and mass spectra, this compound was identified as 7-methoxygeranin A (Figure 2).

Antioxidant Activity of Cassipourea Species Extract

The antioxidant activities of the three *Cassipourea* species are shown in Table 2. The results are presented as the mean values along with the standard deviation obtained from three parallel measurements for each parameter. Raw data is illustrated in Table S2. The total polyphenol and flavanol content ranged between 97.91 and 143.68 (mg GAE/g) and 6.58 and 14.67 (mg QE/g), respectively, for all extracts, with *C. gummiflua* extract having the highest in both cases ($p < 0.001$). Similarly, *C. gummiflua* extract had the highest FRAP (526.07 AAE/g), DPPH (390.26 TE/g) and TEAC (596.98 TE/g), followed by *C. malosana* and *C. flanaganii* (Table 2).

The ANOVA results revealed significant main effects of both plant extracts ($\eta 2p=0.600$) and assay type ($\eta 2p=0.959$) (Table S3) on antioxidant activity ($p<0.001$). Post-hoc analyses (Table S4) indicated significant differences in antioxidant activity between Plant Code 2020 (*C. gummiflua*) and both 2021 (*C. malosana*) and 2022 (*C. flanaganii*) ($p<0.001$), but not between 2021 (*C. malosana*) and 2022 (*C. flanaganii*) ($p=0.883$).

Assay comparisons (Table S5) showed significant differences across most pairs, except for FRAP vs TEAC ($p=0.668$) and Flavonols (Flav1) vs Flavanols (Flav2) ($p=0.591$), underscoring the critical role of assay selection in antioxidant activity measurements (Figure 3). Despite violations of homogeneity (Table S6) of variances ($p<0.001$), the robust ANOVA results highlight the substantial influence of plant source and assay type on antioxidant activity outcomes, emphasizing the need for standardized protocols and consideration of sample variability in future studies. These results suggest that *C. gummiflua* consistently exhibits higher antioxidant activity across all measures than *C. malosana* and *C. flanaganii*, which showed lower but comparable levels of antioxidant properties.

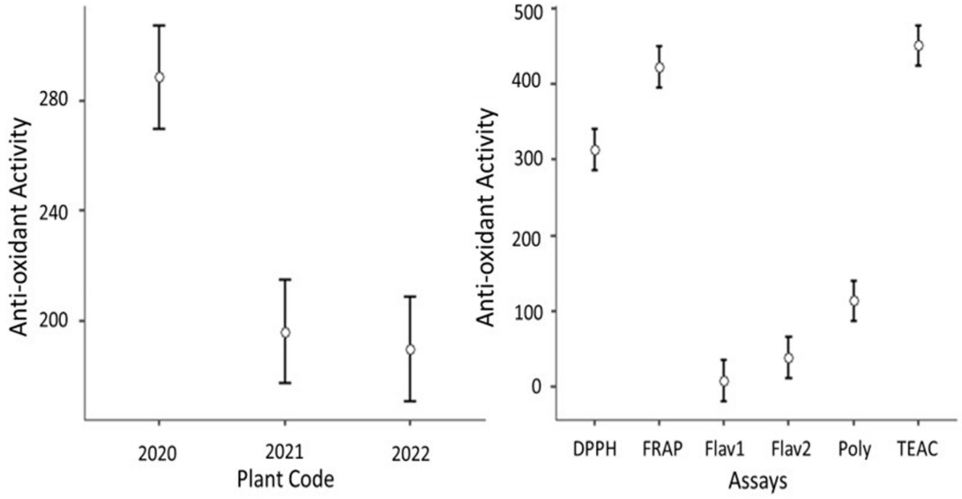


Figure 3 Plot of the Estimated Marginal Means for Plant Code and Assays.

Table 3 IC_{50} of Three Cassipourea Species and Isolated Compound

Extracts	IC_{50} (µg/mL) ± SD
C. malosana	87.47 ± 1.52
C. flanaganii	37.10 ± 1.17
C. gummiflua	57.65 ± 1.28
7-methoxygeranin A	45.16 ± 1.45
Kojic acid	3.95 ± 0.087

Anti-Tyrosinase Activities of Cassipourea Species Extracts

The three ethanolic extracts of *Cassipourea* species, including one compound (7-methoxygeranin A) isolated from *C. malosana,* were evaluated for tyrosinase inhibitory activity at different concentrations (Table S7). The three extracts were observed to inhibit tyrosinase by over 30% and 60% at 100 µg/mL and 1000 µg/mL (the highest concentration investigated), respectively. On the other hand, 7-methoxygeranin A (65.49%) had a lesser inhibitory effect at 1000 µg/mL relative to the three extracts. Extract from *C. flanaganii* with an IC_{50} (inhibitory concentration, 50%) value of 37.10 µg/mL, which was lower compared to that observed for 7-methoxygeranin A (45.16 µg/mL) was the most active among the extracts. The two other extracts from *C. gummiflua* and *C. malosana* showed moderate activity against tyrosinase with IC_{50} values of 57.65 and 87.47 µg/mL, respectively. Kojic acid, a well-known tyrosinase inhibitor, was used as the standard and had an IC_{50} value of 3.95 µg/mL (Table 3).

The ANOVA results revealed no significant main effect of *Cassipourea* species or isolated compounds on tyrosinase inhibition (F (4, 25) = 0.602, p = 0.665, η^2p = 0.088), (Table S8) indicating comparable inhibitory activity across extracts (Figure 4). Homogeneity of variances was confirmed ($p > 0.05$), and post-hoc comparisons (Table S9) showed no significant differences between any pairs of extracts ($p > 0.05$). However, a significant main effect of solution concentration (Table S10) on inhibition was observed ($F(9, 20) = 6.08$, $p < 0.001$, $\eta^2p = 0.732$), with higher concentrations (eg, 1000 µg/mL) (Table S11)

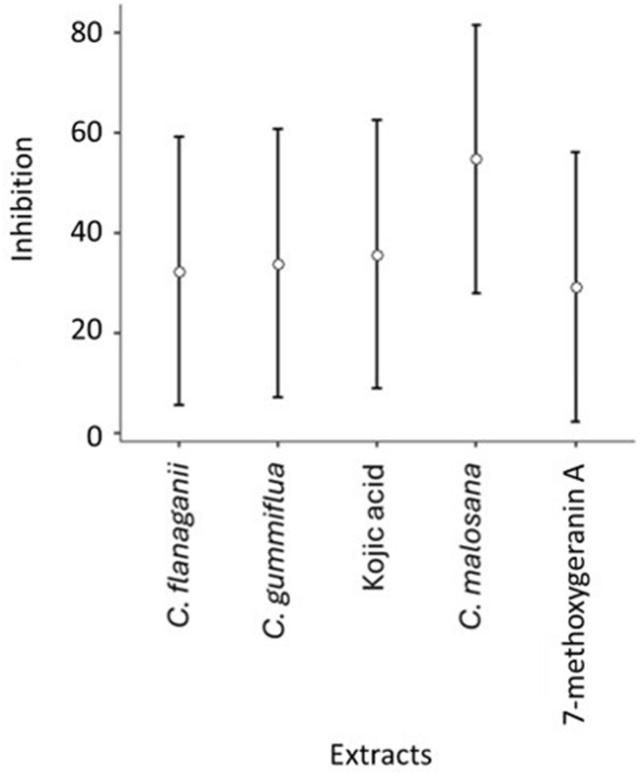


Figure 4 Plot of the Estimated Marginal Means for Extract types.

https://doi.org/10.2147/JEP.S504759

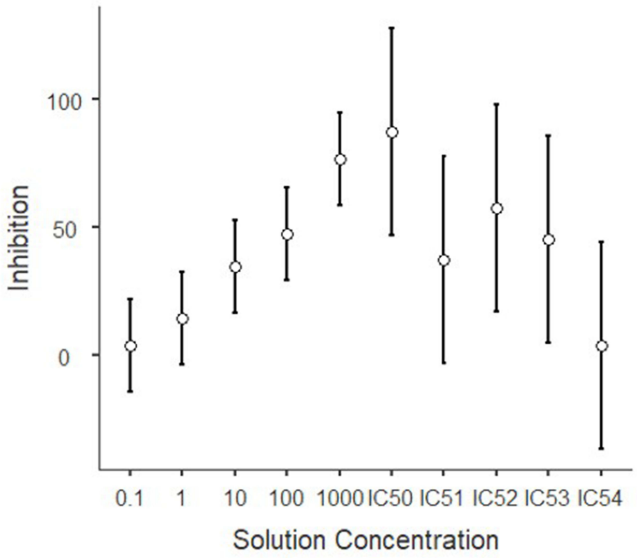


Figure 5 Plot of the Estimated Marginal Means for Solution Concentrations.

demonstrating significantly greater inhibition (Figure 5) compared to lower concentrations (eg, 0.1 µg/mL, $p < 0.001$). These findings highlight the concentration-dependent nature of tyrosinase inhibition, emphasizing the importance of optimizing solution concentrations for effective inhibition. Further studies are needed to explore additional factors influencing tyrosinase activity and to validate these findings in broader contexts.

In Silico Screening of Top-Five Metabolites

The pharmacokinetic properties and docking score values of the *Cassipourea* metabolites are presented in Table 4. Except for azelaic acid (−4.5 kcal/mol), all the investigated Cassipourea metabolites had lower docking scores than the standard (−4.8 kcal/mol) with ent-atis-16-en-19-oic acid having the lowest score (−7.9 kcal/mol). Azelaic acid was excluded from the further screening. Interestingly, these metabolites demonstrated varying ADMET and toxicity properties. Except in five metabolites (ent-atis-16-en-19-oic acid, isorhamnetin 3-*O*-rhamnoside, lupeol stearate, lyoniside, and 7-methoxygeranin), all the identified metabolites of *Cassipourea* species passed the Lipinski's Ro5. The metabolites had lower toxicity profiles relative to the standard (LD_{50} of 550 mg/kg and toxicity class 3) with moderate to high water solubility, except for lupeol stearate (Table 4). Except for five compounds (*Ent*-atis-16-en-19-oic acid, isorhamnetin 3-*O*-rhamnoside, emodin 6,8-dimethyl ether, ellisinin A, tricin, and 7-methoxygeranin A), all metabolites were non-inhibitors of cytochrome P3A4. Taken together, the Lipinski Ro5 (with 0 violation) was used as the hallmark for the selection of the top five metabolites subsequently taken for MD simulation analysis. Similarly, the top five metabolites were readily bioavailable and absorbed gastrointestinally, with no end-point/organ toxicities (except emodin 6,8-dimethyl ether, which showed potential immunotoxicity and mutagenicity). Additionally, the metabolites possessed LD_{50} and toxicity classes of ≥2500 mg/kg and 5, respectively (Table 4).

The energy framework of the top-ranked *Cassipourea* metabolite-tyrosinase complexes is shown in Table 5 with the metabolites exhibiting significantly lower ΔG_{bind} than the reference standard (–5.14±6.25 kcal/mol). Of the top five metabolites, emodin 6,8-dimethyl ether (−39.88±2.67 kcal/mol) had the lowest ΔG_{bind} while ellisinin A had the highest (−15.22±3.35 kcal/mol) (Table 5).

The post-dynamic trajectories depicting the RMSD, RMSF, ROG, SASA, and the number of H-bond patterns of the bound complexes are presented in Figure 6. The RMSD plot showed an initial equilibration of the bound complexes, which was sustained for approximately 50 ns before the hexose complex diverged slightly from the other bound complexes (Figure 6a). Consequently, the hexose-tyrosinase complex had the highest mean RMSD value (2.09±0.37

Table 4 Docking Score and ADMET Properties of the Selected Top-Scoring Compounds Docked Against Tyrosinase

Ligands	DS (kcal/mol)	MW < 500 (g/mol)	HBA ≤ 10	HBD ≤ 5	Log P o/w≤ 5	WS	GI Abs	BBB P	Pgp	CYP1A2	CYP2C19	CYP2C9	CYP2D6	CYP3A4	LV (N)	BS	H	C	IM	M	C	LD50 (mg/kg)/TC
Ent-atis-16-en-19-oic acid	−7.9	544.51	10	7	2.37	MS	Low	No	No	No	No	Yes	No	Yes	2	0.17	In	In	In	In	In	2500/5
Lupeol	−7.7	426.72	1	1	7.26	PS	Low	No	No	No	No	No	No	No	1	0.55	In	In	Ac	In	In	2000/4
Isorhamnetin 3-O-rhamnoside	−7.4	462.4	11	6	0.64	S	Low	No	Yes	No	No	No	No	Yes	2	0.17	In	In	Ac	In	In	5000/5
Sitosterol glycoside	−7.2	576.85	6	4	5.51	MS	Low	No	No	No	No	No	No	No	1	0.55	In	In	Ac	In	In	8000/6
Lupeol stearate	−6.6	693.18	2	0	13.02	IS	Low	No	Yes	No	No	No	No	No	2	0.17	In	In	Ac	In	In	339/4
Chrysin 8-C-glucoside	−6.5	416.38	9	6	0.42	S	Low	No	No	No	No	No	No	No	1	0.55	In	In	In	Ac	In	832/4
Chlorogenic acid	−6.5	354.31	9	6	−0.38	S	Low	No	No	No	No	No	No	No	1	0.11	In	In	Ac	In	In	5000/5
Lyoniside	−6.3	552.57	12	6	1.02	S	Low	No	Yes	No	No	No	No	No	3	0.17	In	In	Ac	In	Ac	600/4
Emodin 6,8-dimethyl ether	−6.3	298.29	5	1	2.60	MS	High	Yes	No	Yes	Yes	Yes	No	Yes	**0**	0.55	In	In	Ac	Ac	In	5000/5
Afzelechin	−6.3	274.27	5	4	1.17	S	High	No	Yes	No	No	No	No	No	**0**	0.55	In	In	In	In	In	2500/5
Decahydroretinol	−6.3	286.45	1	1	5.04	S	High	Yes	No	Yes	No	Yes	No	No	1	0.55	In	In	In	Ac	In	1510/4
Ellisinin A	−6.2	266.33	2	2	4.10	MS	High	Yes	No	Yes	No	Yes	Yes	Yes	**0**	0.55	In	In	In	In	In	2830/5
Tricin	−6.1	330.29	7	3	2.15	MS	High	No	No	Yes	No	Yes	Yes	Yes	**0**	0.55	In	In	In	In	In	4000/5
Cassipourol	−5.3	294.52	1	1	5.61	MS	High	No	No	No	No	Yes	Yes	No	1	0.55	In	In	In	In	In	5000/5
Hexose	−5.0	180.16	6	5	−2.26	S	Low	No	Yes	No	No	No	No	No	**0**	0.55	In	In	In	In	In	23000/6
Methyl linoleate	−4.8	294.47	2	0	5.69	MS	High	No	No	Yes	No	Yes	No	No	1	0.55	In	In	In	In	In	20000/6
Azelaic acid	−4.5	188.22	4	2	1.49	S	High	Yes	No	No	No	No	No	No	0	0.85	In	In	In	In	In	900/4
7-methoxygeranin	−7.8	558.53	10	6	2.73	PS	Low	No	No	No	No	Yes	No	Yes	2	0.17	In	In	Ac	In	In	2500/5
Kojic acid	−4.8	142.11	4	2	−0.16	S	High	No	No	No	No	No	No	No	**0**	0.55	In	Ac	In	Ac	In	550/3

Abbreviations: DS, Docking score; MW, Molecular weight; BBB permeant, blood-brain barrier permeation; HB-D, Hydrogen bond donor; Log P o/w, partition coefficient; HB-A, Hydrogen bond acceptor; CY, Cytotoxicity; Pgp, Permeability glycoprotein substrate; WS, Water solubility; CYP, Cytochrome; LV, Lipinski violation; BS, Bioavailability score; H, Hepatotoxicity; C, Carcinogenicity; IM, Immunotoxicity; GI abs, Gastrointestinal absorption; M, Mutagenicity; LD, Lethal dose; TC, Toxicity class; S, Soluble; PS, Poorly soluble; MS, Moderately soluble; IS, Insoluble; Ac, Active; In, Inactive; N, Number of violation.

https://doi.org/10.2147/JEP.S504759

Table 5 MMGBSA-Based Binding Free Energy Framework of Cassipourea Metabolites-Tyrosinase Complexes

Energy Framework (kcal/mol)					
Tyrosinase					
Complex	**ΔE_{vdW}**	**ΔE_{elec}**	**ΔG_{gas}**	**ΔG_{solv}**	**ΔG_{bind}**
Afzelechin	−23.35±6.42	−14.33±9.33	−37.68±12.93	17.78±7.78	−19.90±6.89
Emodin 6,8 dimethyl ether	−46.45±2.38	−9.66±2.00	−56.12±3.04	16.23±1.62	−39.88±2.67
Hexose	−17.64±4.87	−61.88±11.61	−79.52±8.85	50.82±7.96	−28.70±4.19
Tricin	−27.88±3.25	−25.69±6.81	−53.58±8.04	27.50±5.21	−26.08±4.04
Ellisinin A	−19.61±2.79	−4.44±5.94	−24.06±6.21	8.83±3.64	−15.22±3.35
Kojic acid	−6.50±6.51	−6.04±9.04	−12.53±14.09	7.39±8.63	−5.14±6.25

Notes: ΔE_{vdW} = van der Waals energy; ΔE_{elec} = electrostatic energy; ΔE_{gas} = gas-phase free energy; ΔG_{sol} = solvation free energy; ΔG_{bind} = total binding free energy.

Å), while the other metabolite complexes were not significantly different from the apo-enzyme (1.80±0.26 Å) with the standard complex (kojic acid-tyrosinase) having the least mean value (1.65±0.18 Å) (Table 5).

For the RMSF plot, minimal peak vibrations were recorded for amino acid residues. However, prominent fluctuations were observed between 200 and 250 amino acid residues with tricin-tyrosinase and emodin 6,8 dimethyl ether-tyrosinase complexes, with the highest fluctuations in this region (Figure 6b). Except for afzelechin- and hexose-tyrosinase complexes, all the other bound complexes had lower mean RMSF values relative to the apo-enzyme (1.15±0.63 Å) with kojic acid having the lowest value (1.08±1.68 Å) (Table 5).

Although the afzelechin-tyrosinase complex fluctuated slightly around 20 and 30 ns in the ROG plot, a stable plot was observed for the complex at the end of the 150 ns simulation (Figure 6c). Tricin-complex (20.69±0.07 Å) on the other

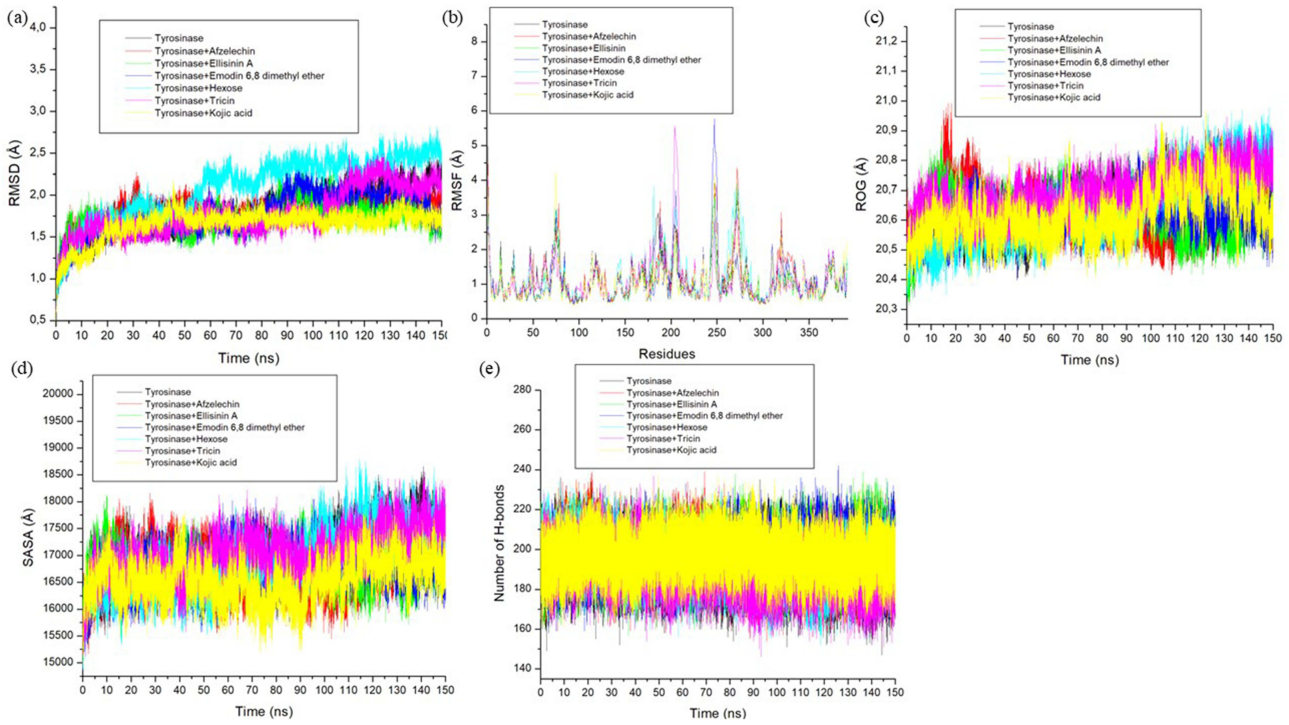


Figure 6 Comparative post-dynamic (**a**) RMSD, (**b**) RMSF, (**c**) ROG, (**d**) SASA and (**e**) number of intramolecular hydrogen bonds after 150 ns MD simulations period.

Table 6 Mean RMSD, RMSF, ROG, SASA, and Hydrogen Bonds of Apo-Enzyme, Cassipourea Metabolites, and the Standard Against Tyrosinase

Complex	Mean RMSD (Å)	Mean RMSF (Å)	Mean ROG (Å)	Mean SASA (Å)	Mean Number of H-Bonds
Apo-tyrosinase	1.80±0.26	1.15±0.63	20.65±0.07	16,969.35±434.03	192.03±9.73
Tyrosinase					
Afzelechin	1.79±0.17	1.23±0.96	20.63±0.07	16,758.47±372.24	194.35±9.89
Emodin 6,8 dimethyl ether	1.79±0.25	1.10±0.85	20.61±0.06	16,791.73±351.61	196.69±9.19
Hexose	2.09±0.37	1.24±0.93	20.64±0.11	16,938.01±552.44	192.94±9.84
Tricin	1.78±0.27	1.12±0.65	20.69±0.07	17,015.00±418.90	190.84±9.86
Ellisinin A	1.74±0.17	1.06±0.64	20.62±0.06	16,805.08±302.73	197.18±9.27
Kojic acid	1.65±0.18	1.08±1.68	20.62±0.08	16,546.24±364.18	197.53±9.33

hand showed slightly higher mean ROG value compared to the other bound complexes (including kojic acid) which had mean values that were not significantly different from one another (Table 5). Similarly, a stable SASA plot that fluctuated between 15500 and 18500 was observed for the bound complexes throughout the 150 ns simulation (Figure 6d). While the tricin-tyrosinase complex (17015.00±418.90 Å) showed a higher mean SASA value than the apo-gene (16969.35 ±434.03 Å), other metabolites and standard bound complexes were lower (Table 5).

The number of H-bonds plot was stable throughout the simulation with the kojic acid-tyrosinase complex showing a broader pattern between 220 and 170 h-number relative to the metabolite-bound complexes (Figure 6e). Except for the tricin-tyrosinase complex, all the metabolites had higher H-number than the apo-enzyme (192.03±9.73) while among the metabolites, ellisinin A (197.18±9.27) had the highest mean H-number followed by the standard and emodin 6,8-dimethyl ether (196.69±9.19) (Table 6).

The 2D interaction plots of the top five *Cassipourea* metabolites and the standards are presented in Figure 7. Except for the hexose-tyrosinase complex, reductions in the total number of interactions formed were observed during the 150 ns MD simulation. With the afzelechin-tyrosinase complex, the 12 interactions (comprising 3 h-bonds; Glu43, Asn173, and Hie177) formed at the beginning of the simulation reduced to 11 [3 new H-bonds (Ala249, Trp226, and Asn252)] at 150 ns (Figure 7). The initial 16 interactions including 4 h-bonds (Thr307, Tyr310, Glu355, and Asp356) observed in tyrosinase-emodin 6,8- dimethyl ether complex reduced to 14 with 3 h-bonds (Met7, Pro8, and Gly11) after 150 ns MD simulation (Figure 7). Hexose complex with tyrosinase had 9 interactions including 2 h-bond (Lys375 and Glu355) at 0 ns and 10 total interactions including H-bonds with Asp356, Gln306, and Lys378 at 150 ns (Figure 7). The 15 interactions (including 5 h-bonds) of the tricin-tyrosinase complex were reduced to 11 interactions with 2 h-bonds after 150 ns MD simulation (Figure 7). The initial 10 interactions including 2 h-bonds (Hie83 and Glu255) observed in tyrosinase-ellisinin A complex were reduced to 8 with no H-bonds at the end of 150 ns MD simulation (Figure 7), while kojic acid-tyrosinase complex with 13 interactions including 8 h-bonds at 0 ns had 8 interactions with 2 h-bonds after 150 ns MD simulation (Figure 7).

Discussion

In this study, in vitro and in silico approaches were used to explore the anti-tyrosinase potential and free radical scavenging capabilities of three *Cassipourea* species for the treatment of melasma. Melasma is a disfiguring chronic skin condition characterized by excessive melanin production in areas exposed to UV radiation. Due to its complex etiology with multiple pathologies, including photoaging, excessive melanogenesis, increased mast cell count, vascularization, and basement membrane damage, melasma is challenging to manage.[43–45] Due to its visibility, melasma is often associated with negative emotional and mental health, which may lead to anxiety, depression, suicidal ideation, low self-esteem, and embarrassment.[43,45,46]

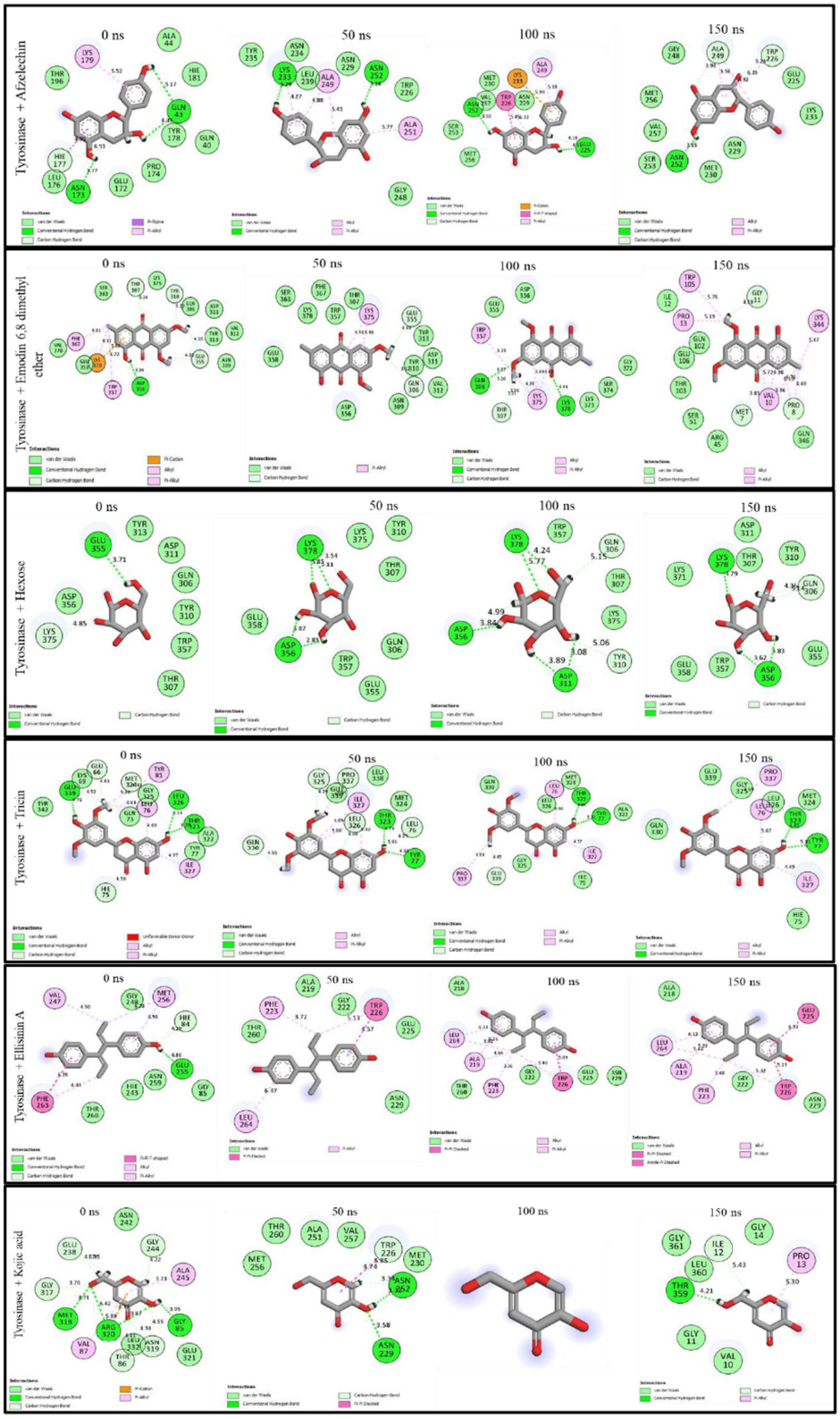


Figure 7 2D interaction plots of the afzelechin-, emodin 6,8 dimethyl ether-, hexose-, tricin, ellisinin A- and kojic acid- tyrosinase complexes over 150 ns MD simulation.

The melasma treatment plan usually begins with the elimination of risk factors, strict protection against UV radiation and visible light, and the use of topical lightening agents.[43,47] Traditionally, melasma is treated with topical agents such as hydroquinone, tretinoin, glucocorticoids, and formulations, however, these treatment modalities can exfoliate and irritate the skin barrier resulting in skin irritation, pruritus, and redness which in turn aggravates skin inflammation leading to vascular complexities, while on the contrary, botanicals are often better tolerated as they repair the inflammation and remodel the skin barrier.[46] The current combination therapy approach involves topical application, chemical peels, the use of lasers and lights, mesotherapy, micro-needling, and systemic therapy.[43] Treatment of melasma requires long-term commitment and can lead to recurrence and resistance. Melasma treatment involves the inhibition of melanin synthesis, reduction of melanosome transfer to keratinocytes, and acceleration of melanin removal pathways.[43]

In rural areas of KwaZulu-Natal and Eastern Cape Provinces, women use the crude bark of three *Cassipourea* plants (*Cassipourea flanaganii, Cassipourea malosana, Cassipourea germiflua*) interchangeable for their skin-lightening effects as well as for sun protection.[16] Traditional local names are used interchangeably. Hence, in this study, possible differences between the three *Cassipourea* plant species concerning their potential antioxidant and anti-tyrosinase activities were investigated.

Antioxidant Activities of Cassipourea Species

Antioxidants neutralize free radicals, which are highly reactive molecules that can damage skin cells and contribute to various skin conditions, including hypermelanosis disorders, such as melasma. Thus, incorporating antioxidants into melasma management therapy may enhance existing treatments and improve treatment outcomes for melasma, thereby resulting in desired optimal results.[13] In this study, the higher total polyphenol and flavanol contents observed in *C. gummiflua* extract relative to the extracts from the two other *Cassipourea* species investigated suggest that *C. gummiflua* might have better antioxidant properties. Previous studies have established a good correlation between phenolic content and antioxidant properties.[48,49] Interestingly, the higher total polyphenol and flavanol contents observed with *C. gummiflua* extract were statistically different when subjected to different statistical models, including ANOVA and post-hoc comparisons, suggesting a clear difference in the total phenolic content of the three species of *Cassipourea* investigated. This clear difference in the phenolic content of the plant species was observed to have no significant effect on the anti-tyrosinase activities observed in this study but was noted to have an impact on their antioxidant effects. This is obvious as *C. gummiflua* extract with the highest polyphenol and flavanol contents scavenges higher DPPH with higher FRAP and TEAC activities, all pointing to higher antioxidant properties. *C. malosana* with the second-highest total polyphenol and flavanol contents had the second-best antioxidant properties. These observations are in tandem with those of previous studies, where higher total phenolic content translated to better antioxidant activities.[8,9] Furthermore, 7-methoxygeranin A has been reported to improve skin health owing to its known antioxidant effects.[42] Thus, its successful isolation from *C. malosana* coupled with its anti-tyrosinase effect in this study provides slight evidence for its use in skincare. Despite the potential benefits of 7-methoxygeranin A for skin health, including its possible role in managing melasma, it is essential to note that more studies are needed to fully understand its mechanism of action. Additionally, the efficacy of 7-methoxygeranin A may depend on factors such as its concentration, formulation, and mode of administration (eg, topical application vs oral supplementation). Hence, further research is needed to determine the optimal use of 7-methoxygeranin A for melasma, and to assess its safety and potential side effects. To ascertain whether 7-methoxygeranin A, which has been reported to have good skin care potential, is the lead compound in *Cassipourea* species, this study computationally screened all the reported metabolites of *Cassipourea* species against tyrosinase.

Anti-Tyrosinase Activities of the Cassipourea Species

By targeting tyrosinase and melanin synthesis, tyrosinase inhibitors effectively lighten hyperpigmented areas and reduce skin tone in conditions such as melasma. In this study, no significant difference ($F(4, 25) = 0.602$, $p = 0.665$, $\eta^2p = 0.088$) was observed in the anti-tyrosinase activities of the three *Cassipourea* species extracts and 7-methoxygeranin A. This suggested that the different *Cassipourea* species and 7-methoxygeranin A did not significantly differ in their ability to inhibit tyrosinase activity. However, descriptive analysis illustrated that *C. flanaganii* might be slightly better than the other two plants and 7-methoxygeranin. Homogeneity of variance tests indicated no significant differences among the treatments according to Levene's[50] ($F(4, 25) = 2.43$, $p = 0.074$) and Bartlett's tests[33] ($\chi^2(4) = 2.64$, $p = 0.620$), suggesting

that the assumption of homogeneity of variance was met. The assumption of variance homogeneity is perhaps reflected in the indifference of indigenous people in this region towards the efficacy of various plant-based cosmetics or dermatological interventions,[46] suggesting a consistent perspective across the population. The post hoc comparisons also showed no difference ($P > 0.05$) in the anti-tyrosinase activities of the three extracts.

In Silico Identification of Lead Metabolites from Cassipourea Species

Based on the findings obtained from the in vitro study, the potential anti-tyrosinase mechanism of *Cassipourea metabolites* considered to be responsible for this effect was further investigated to identify lead compounds with potential in skin hyperpigmentation treatment. To this end, in silico techniques, such as molecular docking and MD simulations, which help in the identification of active lead molecules from a library of compounds, were carried out.[51] Molecular docking serves as an initial screening tool that provides information on the binding interaction and fitness of a ligand in the binding pocket of a protein with a higher negative docking score, depicting greater binding orientation and interaction.[52] Except for azelaic acid, which had a higher negative docking score than the standard, all other investigated *Cassipourea* metabolites displayed lower docking scores, suggesting a better binding fitness and orientation with tyrosinase. Since this study sought to identify the top druggable anti-tyrosinase metabolites, the metabolites were screened for oral drug-likeness, pharmacokinetics, and toxicity. Although all the metabolites displayed remarkably good drug-like properties, only afzelechin, emodin 6,8-dimethyl ether, hexose, tricin, and ellisinin A were used for MD simulation because of their exceptional oral bioavailability properties, as suggested by their zero violation of Lipinski Ro5. What is notable at this stage is the absence of 7-methoxygeranin A in the identified top-ranked compounds (premised on pharmacokinetic concerns), which suggests the presence of other lead metabolites with anti-tyrosinase activities and better pharmacokinetic profiles in *Cassipourea* species.

Using MD simulations, detailed information on the stability, compactness, and flexibility of a complex can be obtained, enabling the identification of active molecules.[53] ΔG_{bind} is an energy component indicator that describes the binding affinity of a ligand in the binding pocket of a protein. The lower the ΔG_{bind} the greater the binding affinity and pointer to the level of stability of the complex.[54] In this study, the top-ranked metabolites had significantly lower ΔG_{bind} values relative to the standard, suggesting their better potential to bind and inhibit tyrosinase activity. Inactivation of tyrosinase has been shown to have a regulatory effect on melanin production and reduction of hyperpigmentation. Among the top-ranked compounds, emodin 6,8-dimethyl ether exhibited the lowest ΔG_{bind} when bound to tyrosinase, denoting this compound as the lead anti-tyrosinase inhibitor.

Regarding the stability of a bound complex, RMSD was employed to measure the extent of convergence or divergence of the complexes during the simulation.[53] A lower fluctuating RMSD pattern or mean value denotes better binding stability.[55] Comparatively, kojic acid-tyrosinase and ellisinin A-tyrosinase complexes with the lowest RMSD value had the best stability, indicating the advantages of kojic acid and ellisinin A as potential modulators of tyrosinase. However, except for hexose-tyrosinase, the finding that all the bound top-ranked metabolite, standard, and apo-enzyme complexes had negligible differences in their mean RMSD values, which were <3.0 Å, strongly indicated stable complexes for all the systems.[56] This observation is in line with other similar studies that also showed better stability for bound complexes, with a mean RMSD of <3.0 Å.[57]

RMSF measures the flexibility of the amino acid residues of the protein during the simulation, and its evaluation might provide insight into the stability of the intra- and intermolecular bonding of the complex.[58] The higher fluctuation between the 200–250 amino acid region for tricin-tyrosinase and emodin 6,8-dimethyl-tyrosinase during the simulation did not include active site residues such as Pro284, Asn81, Glu322, Gly86, and val283, which are critical for the modulation of tyrosinase, thus indicating strong intermolecular bonding at the active site of the protein during the simulation. Similarly, the observation of a low RMSF value (<3 Å) for all the complexes, including the apo protein, during the simulation indicates less vibration in the complexes and an indication of strong intramolecular binding. Another deduction from this observation is that the binding of the top-ranked metabolite and the standard did not induce thermodynamic disorder in tyrosinase. Consistent with the RMSD findings of this study is the least thermodynamic disorderliness observed with kojic acid-tyrosinase and ellisinin A-tyrosinase complexes with the least RMSF value during the simulation, thus further reinforcing the benefit of kojic acid and ellisinin A as modulators of tyrosinase.

The spatial distribution or compactness of a complex is described by the ROG; the lower the ROG fluctuations, the better the compactness.[59] Interestingly, all bound systems formed compact complexes with negligible differences in their mean ROG values. This observation suggests increased stability for all complexes. The slight differences in the mean ROG values for all the complexes could indicate that the ROG values have little impact on the differential ΔG_{bind} value observed for the top-ranked compound in this study. This observation is consistent with a prior study where the compactness of complexes had a negligible effect on ΔG_{bind}.[59,60] The SASA value measures the changes in protein surface area and the accessibility of the protein surface area to the solvent.[60] The lower the SASA value, the better the binding stability.[61] The observation of a less fluctuating SASA plot in all bound systems might indicate stable complex formation. Similar to the ROG, the slight differences in the mean SASA values for all the complexes could indicate that SASA values have little impact on the differential ΔG_{bind} value observed for the top-ranked compound in this study.

H-bonds are important for the structural stability, reactivity, and interactions.[62] The formation of a non-fluctuating H-bond plot indicates the formation of stable-bound complexes. Apart from tricin, *Cassipourea* metabolite complexes have a higher mean H-bond number relative to the apo-protein, indicating improved structural stability. However, the higher mean number of H-bonds observed with the bonded complexes relative to the apo enzyme might indicate the presence of some intermolecular H-bonds. The highest H-bond was observed for kojic acid-tyrosinase and ellisinin A-tyrosinase complexes. This observation suggests that more intermolecular H-bonds are formed in kojic acid-tyrosinase and ellisinin A-tyrosinase relative to other investigated complexes, which is not only consistent with the RMSD and RMSF findings of this study but also strengthens the potential of kojic acid and ellisinin A as modulators of tyrosinase.

Except for hexose-tyrosinase, a reduced number of interactions was recorded after 150 ns of MD simulation. While this observation might suggest an increase in the inability of the top-ranked metabolite and standard to modulate tyrosinase, it is worth noting that some of the critically important amino acid residues at the active site were retained after the simulation. Thus, these observations demonstrate that the top-ranked compounds have prolonged residence at the active site of the protein to inactivate it, even with less interaction. The smaller number of interactions observed in the kojic acid-tyrosinase complex relative to the top-ranked metabolites denotes better binding interactions between the top-ranked compounds and the enzyme. Since the regulation of tyrosinase activity helps to reduce melasma and hyperpigmentation, the reduced number of H-bonds and the retention of some catalytic amino acids after the long simulation suggest that the interaction of the top-ranked compounds with tyrosinase is stable for the modulation of skin pigmentation. Thus, evidence from in vitro study showed that *Cassipourea* species exhibit anti-tyrosinase and free radical scavenging effects in the regulation of melasma or skin hyperpigmentation, whereas its metabolites, especially emodin 6,8-dimethyl ether, show interesting binding interactions and stability with tyrosinase, which is critical for the inhibition of its activity and regulation of skin hyperpigmentation.

Conclusions

Based on current evidence, extracts from the three *Cassipourea* species showed high anti-tyrosinase and antioxidant activities. Although statistical analysis showed no significant difference in the anti-tyrosinase effects of the three plant extracts, the descriptive analysis showed that the extract of *C. flanaganii*. The total polyphenol and flavanol contents of the extracts were observed to have no significant effect on the anti-tyrosinase activity but were noted to impact their antioxidant effects, as *C. gummiflua*, which had the highest total polyphenol and flavanol content, had the best antioxidant activities. The isolated metabolite (7-methoxygeranin A) was noted to have a lower anti-tyrosinase effect than the most effective extract (*C. flanaganii*). 7-methoxygeranin A is a well-known antioxidant that is used in the management of various skin conditions, including melasma. However, its lower anti-tyrosinase effect suggests the presence of other lead metabolites with greater anti-tyrosinase activity in *Cassipourea* species; hence, the in-silico screening of all metabolites of *Cassipourea* species. Interestingly, the absence of 7-methoxygeranin A in the identified top-ranked compounds due to pharmacokinetic concerns confirmed the curiosity and subsequent MD simulation of the top-ranked compound at the active site of tyrosinase, identified emodin 6,8-dimethyl ether as the lead compound. Emodin 6,8-dimethyl ether was observed to have significant stability while interacting with key amino acids even after 150 ns of MD simulation, suggesting its prolonged residence at the active site of the enzyme for inactivation to take place. However, further in vitro and in vivo studies on the anti-tyrosinase activities of emodin 6,8 dimethyl ether are highly

recommended. Despite the potential benefits of 7-methoxygeranin A for skin health, including its possible role in managing melasma, it is essential to note that more studies are needed to fully understand its mechanism of action.

The investigation of anti-tyrosinase and radical scavenging activities in selected Cassipourea plants holds significant future implications for the development of natural skin lighteners and enhanced photo-protection approaches. These plant extracts could provide safer alternatives to synthetic agents like hydroquinone, addressing hypermelanosis disorders while offering antioxidant benefits against UVR-induced oxidative stress. Furthermore, the results of this research support indigenous knowledge and traditional practices while promoting economic opportunities for local communities through sustainable harvesting. In sum, harnessing the potential of Cassipourea plants aligns with a growing demand for effective, natural skincare solutions for all people in the skin care industry.

Data Sharing Statement

All data is provided in the manuscript.

Ethical Approval

The study was approved by the University of KwaZulu-Natal Biomedical Research Ethics Committee (UKZN BREC) (protocol reference number: BREC/00002721/2021).

Acknowledgments

The authors wish to thank Prof. Neil Crouch from SANBI for identifying the plant material.

This work is based on research supported by the Department of Higher Education and Training (DHET) through the University Capacity Development Programme (UCDP), under the University Staff Development Programme (USDP) funding framework, Phase 5, 2024.

Author Contributions

All authors made a significant contribution to the work reported, whether that is in conception, study design, execution, acquisition of data, analysis and interpretation, or in all these areas; took part in drafting, revising or critically reviewing the article, gave final approval of the version to be published; have agreed on the journal to which the article has been submitted; and agree to be accountable for all aspects of the work.

Disclosure

The authors declare no conflicts of interest in this work.

References

1. Makgobole MU, Onwubu SC, Nxumal CT, Mpofana N, AA-n A. In search of oral cosmetics from nature: a review of medicinal plants for dental care in West Africa. *S Afr J Bot*. 2023;162:644–657. doi:10.1016/j.sajb.2023.09.050
2. WHO. *WHO Expert Committee on Specifications for Pharmaceutical Preparations: Forty-second Report*. World Health Organization. 2008;Vol. 948.
3. Thibane V, Ndhlala A, Abdelgadir H, Finnie J, Van Staden J. The cosmetic potential of plants from the Eastern Cape Province traditionally used for skincare and beauty. *S Afr J Bot*. 2019;122:475–483. doi:10.1016/j.sajb.2018.05.003
4. Mpofana N, Chipangura JK, Paulse M, et al. An Investigation into the Acute and Subacute Toxicity of Extracts of Cassipourea flanaganii Stem Bark In Vivo. *Plants*. 2023;12(12):2281. doi:10.3390/plants12122281
5. Ribeiro AS, Estanqueiro M, Oliveira MB, Sousa Lobo JM. Main benefits and applicability of plant extracts in skin care products. *Cosmetics*. 2015;2 (2):48–65. doi:10.3390/cosmetics2020048
6. Langat MK, Dlova NC, Mulcahy-Ryan LE, et al. The effect of isolates from Cassipourea flanaganii (Schinz) Alston, a plant used as a skin lightning agent, on melanin production and tyrosinase inhibition. *J Ethnopharmacol*. 2021;264:113272. doi:10.1016/j.jep.2020.113272
7. Lall N, Kishore N. Are plants used for skin care in South Africa fully explored? *J Ethnopharmacol*. 2014;153(1):61–84. doi:10.1016/j.jep.2014.02.021
8. Singleton VL, Orthofer R, Lamuela-Raventós RM. Analysis of total phenols and other oxidation substrates and antioxidants by means of folin-ciocalteu reagent. *Methods Enzymol*. 1999;152–178.
9. Mazza G, Fukumoto L, Delaquis P, Girard B, Ewert B. Anthocyanins, phenolics, and color of Cabernet franc, Merlot, and Pinot noir wines from British Columbia. *Journal of Agricultural and Food Chemistry*. 1999;47(10):4009–4017. doi:10.1021/jf990449f
10. Treutter D. Chemical reaction detection of catechins and proanthocyanidins with 4-dimethylaminocinnamaldehyde. *J Chromatogr A*. 1989;467:185–193. doi:10.1016/S0021-9673(01)93963-9

11. Benzie IF, Strain J. Ferric reducing/antioxidant power assay: direct measure of total antioxidant activity of biological fluids and modified version for simultaneous measurement of total antioxidant power and ascorbic acid concentration. *Methods Enzymol*. 1999;15–27.
12. Re R, Pellegrini N, Proteggente A, Pannala A, Yang M, Rice-Evans C. Antioxidant activity applying an improved ABTS radical cation decolorization assay. *Free Radic Biol Med*. 1999;26(9–10):1231–1237. doi:10.1016/S0891-5849(98)00315-3
13. Sharma OP, Bhat TK. DPPH antioxidant assay revisited. *Food Chem*. 2009;113(4):1202–1205. doi:10.1016/j.foodchem.2008.08.008
14. Momtaz S, Mapunya B, Houghton P, et al. Tyrosinase inhibition by extracts and constituents of Sideroxylon inerme L. stem bark, used in South Africa for skin lightening. *J Ethnopharmacol*. 2008;119(3):507–512. doi:10.1016/j.jep.2008.06.006
15. Souza PM, Elias ST, Simeoni LA, et al. Plants from Brazilian Cerrado with potent tyrosinase inhibitory activity. *PLoS One*. 2012;7(11):e48589. doi:10.1371/journal.pone.0048589
16. Mpofana N, Yalo M, Gqaleni N, Dlova NC, Hussein AA. Analysis of Three Species of Cassipourea Traditionally Used for Hypermelanosis in Selected Provinces in South Africa. *Int J Mol Sci*. 2023;25(1):237. doi:10.3390/ijms25010237
17. Daina A, Michielin O, Zoete V. SwissADME: a free web tool to evaluate pharmacokinetics, drug-likeness and medicinal chemistry friendliness of small molecules. *Sci Rep*. 2017;7(1):42717. doi:10.1038/srep42717
18. Drwal M, Banerjee P, Dunkel M, Wettig M, ProTox RP. A web server for the in silico prediction of rodent oral toxicity. *Nucleic Acids Research*. 2014;42(Web Server issue):W53–W58. doi:10.1093/nar/gku401
19. Dallakyan S, Olson AJ. Small-molecule library screening by docking with PyRx. *Chem Biol*. 2015;243–250.
20. Ismaya WT, Rozeboom HJ, Weijn A, et al. Crystal structure of Agaricus bisporus mushroom tyrosinase: identity of the tetramer subunits and interaction with tropolone. *Biochemistry*. 2011;50(24):5477–5486. doi:10.1021/bi200395t
21. Lanrewaju AA, Enitan-Folami AM, Nyaga MM, Sabiu S, Swalaha FM. Metabolites profiling and cheminformatics bioprospection of selected medicinal plants against the main protease and RNA-dependent RNA polymerase of SARS-CoV-2. *J Biomol Struct Dyn*. 2023;1–21.
22. Nair PC, Miners JO. Molecular dynamics simulations: from structure function relationships to drug discovery. *Silico Pharmacol*. 2014;2(1):1–4. doi:10.1186/s40203-014-0004-8
23. Gonnet P. P-SHAKE: a quadratically convergent SHAKE in O (n2). *J Comput Phys*. 2007;220(2):740–750. doi:10.1016/j.jcp.2006.05.032
24. Seifert E. OriginPro 9.1: scientific data analysis and graphing software-software review. *J Chem Inf Model*. 2014;54(5):1552. doi:10.1021/ci500161d
25. Biovia DS. Discovery Studio, version 21.1. 0. *San Diego: Dassault Systèmes*. 2021;627:1.
26. Csepregi K, Neugart S, Schreiner M, É H. Comparative evaluation of total antioxidant capacities of plant polyphenols. *Molecules*. 2016;21(2):208. doi:10.3390/molecules21020208
27. Amorati R, Valgimigli L. Methods to measure the antioxidant activity of phytochemicals and plant extracts. *Journal of Agricultural and Food Chemistry*. 2018;66(13):3324–3329. doi:10.1021/acs.jafc.8b01079
28. Gülçın İ, Oktay M, Kıreçcı E, Küfrevıoğlu Öİ. Screening of antioxidant and antimicrobial activities of anise (Pimpinella anisum L.) seed extracts. *Food Chem*. 2003;83(3):371–382. doi:10.1016/S0308-8146(03)00098-0
29. Boston JR, Rudy TE, Kubinski JA. Multiple statistical comparisons: fishing with the right bait. *J Crit Care*. 1991;6(4):211–220. doi:10.1016/0883-9441(91)90021-K
30. Brophy AL. A BASIC program for Tukey's multiple comparison procedure. *Behav Res Methods Instrum Comput*. 1984;16(1):67–68. doi:10.3758/BF03201055
31. Zwierzchowska A, Sadowska-Krępa E, Głowacz M, Mostowik A, Maszczyk A. Comparison of designated coefficients and their predictors in functional evaluation of wheelchair rugby athletes. *J Hum Kinet*. 2015;48(1):149–156. doi:10.1515/hukin-2015-0101
32. Jayalath KP, Ng HKT, Manage AB, Riggs KE. Improved tests for homogeneity of variances. *Commun Stat Simul Comput*. 2017;46(9):7423–7446. doi:10.1080/03610918.2016.1241404
33. Arsham H, Lovric M. Bartlett's Test. *Int Encyclopedia Statistical Sci*. 2011;2:20–23.
34. Aloe AM, Thompson CG. The synthesis of partial effect sizes. *Journal of the Society for Social Work and Research*. 2013;4(4):390–405. doi:10.5243/jsswr.2013.24
35. Lakens D. Calculating and reporting effect sizes to facilitate cumulative science: a practical primer for t-tests and ANOVAs. *Frontiers in Psychology*. 2013;4:62627. doi:10.3389/fpsyg.2013.00863
36. Pierce CA, Block RA, Aguinis H. Cautionary note on reporting eta-squared values from multifactor ANOVA designs. *Educ Psychol Meas*. 2004;64(6):916–924. doi:10.1177/0013164404264848
37. Jones M, Hockey R, Mishra GD, Dobson A. Visualising and modelling changes in categorical variables in longitudinal studies. *BMC Med Res Method*. 2014;14(1):1–8. doi:10.1186/1471-2288-14-32
38. Kim TK. Understanding one-way ANOVA using conceptual figures. *Korean J Anesthesiol*. 2017;70(1):22. doi:10.4097/kjae.2017.70.1.22
39. Larson MG. Analysis of variance. *Circulation*. 2008;117(1):115–121. doi:10.1161/CIRCULATIONAHA.107.654335
40. Baguley T. Calculating and graphing within-subject confidence intervals for ANOVA. *Behavior Research Methods*. 2012;44(1):158–175. doi:10.3758/s13428-011-0123-7
41. Drewes SE, Taylor CW. Methylated A-type proanthocyanidins and related metabolites from Cassipourea gummiflua. *Phytochemistry*. 1994;37(2):551–555. doi:10.1016/0031-9422(94)85098-4
42. Takou DM, Waffo AFK, Langat MK, et al. Melanin Production Inhibitors from the West African Cassipourea congoensis. *Planta Medica Int Open*. 2019;6(02):e50–e56. doi:10.1055/a-1006-2880
43. Piętowska Z, Nowicka D, Szepietowski JC. Understanding melasma-how can pharmacology and cosmetology procedures and prevention help to achieve optimal treatment results? A narrative review. *Int J Environ Res Public Health*. 2022;19(19):12084. doi:10.3390/ijerph191912084
44. Guo EL, Wang JV, Geronemus RG, Friedman PM. Combination Treatment Approach to Melasma. *Advn Cosmetic Surg*. 2021;4(1):97–107. doi:10.1016/j.yacs.2021.01.013
45. Mpofana N, Paulse M, Gqaleni N, et al. The Effect of melasma on the quality of life in people with darker skin types living in Durban, South Africa. *Int J Environ Res Public Health*. 2023;20(22):7068. doi:10.3390/ijerph20227068
46. Guo L, Zhang Y, Wu S, Bai M, Tian S, Miao M. Efficacy and safety of adjuvant topical application of botanicals in the treatment of melasma: a systematic review and meta-analysis. *Heliyon*. 2024;2024:2.

47. Rajanala S, Maymone MB, Vashi NA. Melasma pathogenesis: a review of the latest research, pathological findings, and investigational therapies. *Dermatol Online J*. 2019;25(10). doi:10.5070/D32510045810
48. Muflihah Y, Gollavelli G, Ling Y. Correlation Study of Antioxidant Activity with Phenolic and Flavonoid Compounds in 12 Indonesian Indigenous Herbs. *Antioxidants*. 2021;10(10):1530. doi:10.3390/antiox10101530
49. Kumar S, Sandhir R, Ojha S. Evaluation of antioxidant activity and total phenol in different varieties of Lantana camara leaves. *BMC Res Notes*. 2014;7(1):1–9. doi:10.1186/1756-0500-7-560
50. W-y L. Some modifications of Levene's test of variance homogeneity. *J Stat Comput Simul*. 1987;28(3):213–226. doi:10.1080/00949658708811030
51. Ibrahim SO, Lukman HY, Zubair MF, et al. An Insight into the Physicochemical, Drug-likeness, Pharmacokinetics and Toxicity Profile of Kigelia africana (Lam) Bioactive Compounds. *Al-Bahir J Engd Pure Sci*. 2024;4(1):4.
52. Pellicani F, Dal Ben D, Perali A, Pilati S. Machine learning scoring functions for drug discovery from experimental and computer-generated protein–ligand structures: towards per-target scoring functions. *Molecules*. 2023;28(4):1661. doi:10.3390/molecules28041661
53. Shode FO, JO-o U, Idowu KA, Sabiu S, Govender KK. Molecular dynamics study on selected bioactive phytochemicals as potential inhibitors of HIV-1 subtype C protease. *Metabolites*. 2022;12(11):1155. doi:10.3390/metabo12111155
54. Hata H, Tran DP, Sobeh MM, Kitao A. Binding free energy of protein/ligand complexes calculated using dissociation Parallel Cascade Selection Molecular Dynamics and Markov state model. *Biophys Physicobiol*. 2021;18:305–316. doi:10.2142/biophysico.bppb-v18.037
55. Childers MC, Daggett V. Insights from molecular dynamics simulations for computational protein design. *Mol Syst Des Eng*. 2017;2(1):9–33. doi:10.1039/C6ME00083E
56. Rosenberg MS. *Sequence Alignment: Methods, Models, Concepts, and Strategies*. Univ of California Press; 2009.
57. Lukman H, Aribisala J, Akoonjee A, Sulyman A, Wudil A, Sabiu S. Modulation of dipeptidyl peptidase IV by Rooibos tea metabolites towards type 2 diabetes care: evidence from molecular dynamics simulation and density functional theory. *Sci Afr*. 2024;24:e02173. doi:10.1016/j.sciaf.2024.e02173
58. Hess B. Convergence of sampling in protein simulations. *Phys Rev E*. 2002;65(3):031910. doi:10.1103/PhysRevE.65.031910
59. S'thebe NW, Aribisala JO, Sabiu S. Cheminformatics bioprospection of sunflower seeds' oils against quorum sensing system of Pseudomonas aeruginosa. *Antibiotics*. 2023;12(3):504. doi:10.3390/antibiotics12030504
60. Mousavi SS, Karami A, Haghighi TM, et al. In silico evaluation of Iranian medicinal plant phytoconstituents as inhibitors against main protease and the receptor-binding domain of SARS-CoV-2. *Molecules*. 2021;26(18):5724. doi:10.3390/molecules26185724
61. Khan S, Fakhar Z, Hussain A, et al. Structure-based identification of potential SARS-CoV-2 main protease inhibitors. *J Biomol Struct Dyn*. 2022;40(8):3595–3608. doi:10.1080/07391102.2020.1848634
62. Jairajpuri DS, Hussain A, Nasreen K, et al. Identification of natural compounds as potent inhibitors of SARS-CoV-2 main protease using combined docking and molecular dynamics simulations. *Saudi J Biol Sci*. 2021;28(4):2423–2431. doi:10.1016/j.sjbs.2021.01.040

Journal of Experimental Pharmacology

Dovepress
Taylor & Francis Group

Publish your work in this journal

The Journal of Experimental Pharmacology is an international, peer-reviewed, open access journal publishing original research, reports, reviews and commentaries on all areas of laboratory and experimental pharmacology. The manuscript management system is completely online and includes a very quick and fair peer-review system. Visit http://www.dovepress.com/testimonials.php to read real quotes from published authors.

Submit your manuscript here: https://www.dovepress.com/journal-of-experimental-pharmacology-journal